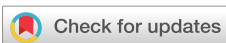


RESEARCH ARTICLE | MARCH 07 2022

Effects of ferromagnetic branch structures on coercivity of alnico permanent magnets

Hoyun Won; Yang-Ki Hong; Minyeong Choi; ... et. al



AIP Advances 12, 035113 (2022)

<https://doi.org/10.1063/9.0000298>



View
Online



Export
Citation

CrossMark

Articles You May Be Interested In

Microstructure and domain studies in Alnico 5 and Alnico 7 (abstract)

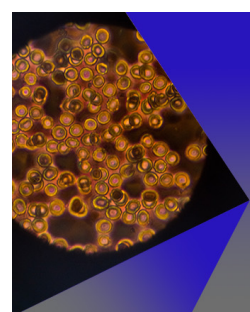
Journal of Applied Physics (April 1985)

Shape and Crystal Anisotropy of Alnico 5

Journal of Applied Physics (May 2004)

On the Alnico Problem

Journal of Applied Physics (June 2004)



AIP Advances

Special Topic: Medical Applications
of Nanoscience and Nanotechnology

Submit Today!

 AIP
Publishing

Effects of ferromagnetic branch structures on coercivity of alnico permanent magnets

Cite as: AIP Advances 12, 035113 (2022); doi: 10.1063/9.0000298

Presented: 27 December 2021 • Submitted: 31 October 2021 •

Accepted: 16 November 2021 • Published Online: 7 March 2022



View Online



Export Citation



CrossMark

Hoyun Won,¹  Yang-Ki Hong,^{1,a)} Minyeong Choi,¹ Gary J. Mankey,² Jongkook Lee,³ Taegyu Lee,³ and Tae Won Lim³

AFFILIATIONS

¹ Department of Electrical and Computer Engineering, The University of Alabama, Tuscaloosa, Alabama 35487, USA

² Department of Physics and Astronomy, The University of Alabama, Tuscaloosa, Alabama 35487, USA

³ Institute of Fundamental and Advanced Technology (IFAT), Hyundai Motor Company, Uiwang-si, Gyeonggi-do, South Korea

Note: This paper was presented at the 15th Joint MMM-Intermag Conference.

a) Author to whom correspondence should be addressed: ykhong@eng.ua.edu

ABSTRACT

The effects of various branches geometry and dimensions such as length, thickness, and width for H-, U-, O-, YH- and YU-shaped alnico structures on coercivity (H_{ci}) using micromagnetic simulation for coherent rotation and curling modes are investigated. The simulation results suggest that the H-shaped structure needs long and short branch length for the coherent rotation and curling, respectively, regardless of branch thickness and width to realize high H_{ci} . Short branch length with thin thickness and short width are recommended for both rotations for the U- and O-shaped structures. Lastly, both Y-shaped structures need branch with long length, thin thickness, and mid-long width for the coherent rotation, but short width for the YH-shaped and mid-long width for the YU-shaped regardless of length and thickness for curling are desired. Furthermore, among the five studied structures, H- or YH-shaped structure for coherent rotation and O-shaped structure for curling are highly recommended for fabrication to realize a high H_{ci} .

© 2022 Author(s). All article content, except where otherwise noted, is licensed under a Creative Commons Attribution (CC BY) license (<http://creativecommons.org/licenses/by/4.0/>). <https://doi.org/10.1063/9.0000298>

I. INTRODUCTION

Due to high saturation magnetization (M_s), small operating temperature coefficient of M_s , and high Curie temperature, alnico permanent magnets (PMs) received much attention.^{1–3} Despite these advantages, its relatively low intrinsic coercivity (H_{ci}) has lessened its market growth in various applications.³

Among reported processes, the thermal-magnetic process (TMP) has achieved the highest H_{ci} of 162 kA/m.² In this process, an external magnetic field is applied along with the casting direction during the annealing process to elongate ferromagnetic FeCo-rich rods (α_1 -phase) embedded in a non-magnetic Al-Ni-rich matrix (α_2 -phase) to increase the shape-anisotropy constant and make the rod end circular, resulting in cylindrical rod.^{1,2} However, during the TMP, an α_1 -phase branch also forms between two α_1 -phase rods and causes H_{ci} to decrease.^{1,4} To observe the effects of such branch on H_{ci} , Ke simulated alnico structure with

two different branch positions on Z-axis using micromagnetic simulation and concluded that the branch connected on the bottom or both bottom and top of the rectangular rod, namely U- and O-shaped structure, showed lower H_{ci} than the branch connected on the middle, namely H-shaped.⁴ Furthermore, Won investigated the effects of various branch geometries and dimensions on H_{ci} for the H- and U-shaped alnico structures having rectangular α_1 -phase rectangular rods and found their optimal branch dimensions.⁵ However, these studies investigated the effect of the branch on the α_1 -phase rectangular rod, not the cylindrical rod, as observed experimentally.^{1,2} Further, the branch can be formed in a Y-shaped structure during the TMP, as reported in Refs. 1 and 2. Thus, this paper investigates the effects of branch length (L_B), thickness (T_B), and width (W_B) on H_{ci} for five structures, including H-, U-, O-, YU-, and YH-structures, using a micromagnetic simulator when α_1 -phase cylindrical rod experiences coherent rotation and curling.

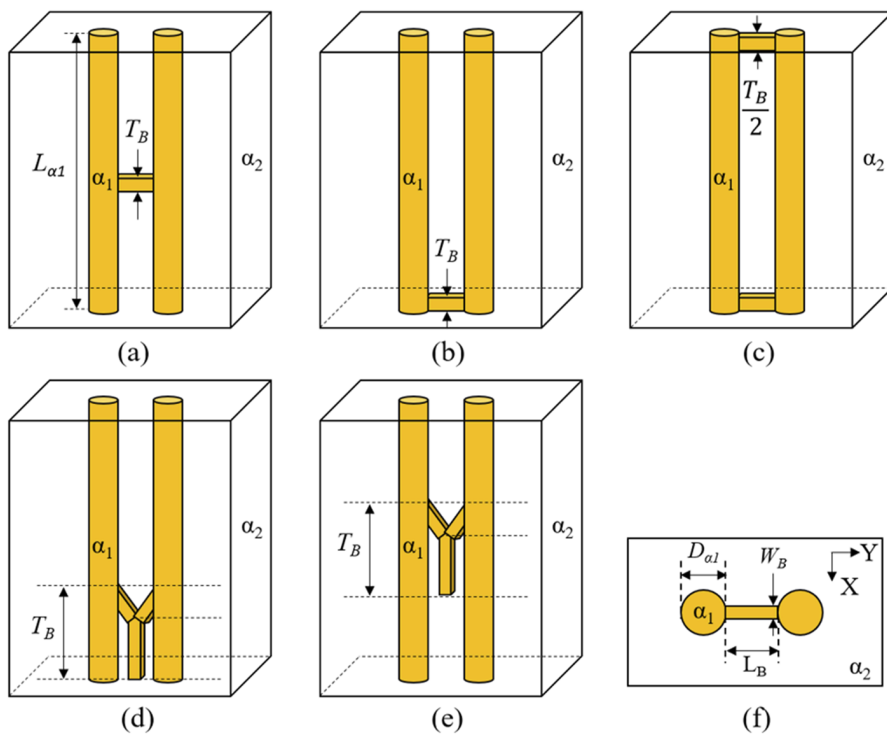


FIG. 1. Alnico structure: Overall view of (a) H-, (b) U-, (c) O-, (d) YU-, and (e) YH-; (f) top view of H-, U-, O-, YU- or YH-.

II. MICROMAGNETIC SIMULATION SETUP

Figure 1 shows the structures of alnico used in the simulation. The alnico element was divided into $1 \times 1 \times 2 \text{ nm}^3$ cell size with an aspect ratio of 8 and simulated with 1 Oe field steps using LLG micromagnetic simulator v2.63b⁶ to obtain M-H hysteresis loop. In this simulation, M_s of 1671 and 0 emu/cc and exchange stiffness (A) of 1.1×10^{-11} and 0 J/m for α_1 - and α_2 -phase are used, respectively.⁵ Two different α_1 -phase diameters ($D_{\alpha 1}$), 10 and 25 nm, were chosen to observe the effects of the rod's spin rotation on H_{ci} . These $D_{\alpha 1}$ are chosen because when $D_{\alpha 1}$ is below 12.8 nm, the coherent rotation dominates, while the curling

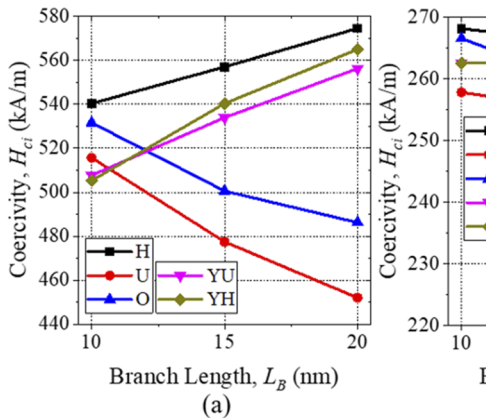
dominates for $D_{\alpha 1}$ above 12.8 nm.¹ For all structures, these effects were observed:

- (i) L_B from 10 to 20 nm at T_B of 30 nm and W_B of 20% of $D_{\alpha 1}$.
- (ii) T_B from 15 to 125 nm at L_B of 15 nm and W_B of 20% of $D_{\alpha 1}$.
- (iii) W_B from 20 to 80% of $D_{\alpha 1}$ at T_B of 30 nm and L_B of 15 nm.

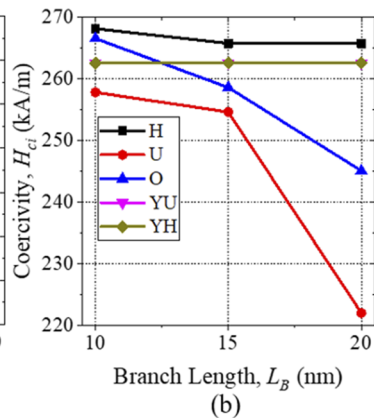
III. RESULTS AND DISCUSSION

A. Branch length

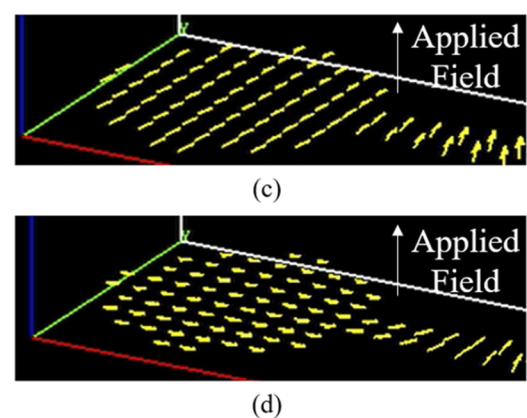
Figure 2 shows the effects of L_B on different structures' H_{ci} , having T_B and W_B listed above for $D_{\alpha 1}$ of 10 and 25 nm. H_{ci} of the



(a)



(b)



(c)

(d)

FIG. 2. H_{ci} versus L_B for $D_{\alpha 1}$ of (a) 10 nm and (b) 25 nm. Surface spin configuration of O-shaped structure with $D_{\alpha 1}$ of 10 nm and L_B of (c) 10 nm and (d) 15 nm.

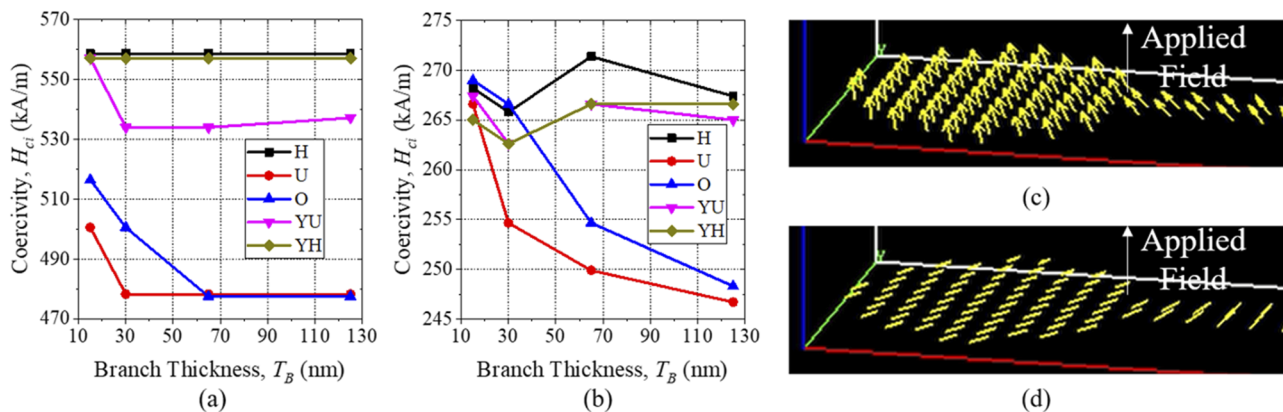


FIG. 3. H_{ci} versus T_B for $D_{\alpha 1}$ of (a) 10 nm and (b) 25 nm. Surface spin configuration of O-shaped structure with $D_{\alpha 1}$ of 10 nm and T_B of (c) 15 nm and (d) 30 nm.

H- and Y-shaped alnico structure increases as L_B increases from 10 to 20 nm, while H_{ci} of other structures decreases for $D_{\alpha 1}$ of 10 nm. For $D_{\alpha 1}$ of 25 nm, a constant H_{ci} of 268.2 and 262.6 kA/m for the H- and Y-shaped structures is observed, respectively. For the U- and O-shaped structures, H_{ci} decreases from 257.8 to 222 kA/m and 266.6 to 245.1 kA/m, respectively. This decrease in H_{ci} for the U- and O-shaped structures is attributed to the in-plane magnetic spin orientation of the cylindrical rods. Compared to the spin orientation in Fig. 2(c), the spin orientation shown in Fig. 2(d) points more perpendicular to the applied field (H_{app}) direction as L_B increases from 10 to 15 nm. H_{ci} increase for the H- and Y-shaped structure is mainly attributed to a 2 % per L_B decrease in exchange energy (E_{ex}).

Accordingly, the simulation result suggests longer L_B for the H- and Y-shaped structures and shorter L_B for the U- and O-shaped structures when the rods experience coherent rotation. For the curling, a shorter L_B is recommended for the U- and O-shaped structure, while any L_B for other structures.

B. Branch thickness

Figure 3 shows the effects of T_B on H_{ci} of five different structures having L_B of 15 nm and W_B of 20% of $D_{\alpha 1}$ when the cylindrical rod experiences coherent rotation and curling. For the H- and YH-shaped structures experiencing coherent rotation, H_{ci} remains constant at 558.7 and 557.1 kA/m, respectively, with respect to T_B . For the others, H_{ci} first decreases and remains constant. The decrease in H_{ci} is mainly attributed to the in-plane spin orientation of the branch, resulting in the in-plane orientation of the cylindrical rods as T_B increases. As illustrated in Fig. 3(c) and (d), the magnetic spin direction of the O-shaped structure having shorter T_B [Fig. 3(c)] is parallel to H_{app} direction, while perpendicular for the structure with longer T_B [Fig. 3(d)]. For curling, although H_{ci} of the H- and Y-shaped structure shows fluctuation, since fluctuation is only 1-2%; H_{ci} can be assumed constant with respect to T_B . For the U- and O-shaped structures, H_{ci} decreases from 257.8 and 266.6 kA/m to 222.1 and 245.1 kA/m, respectively. This decrease

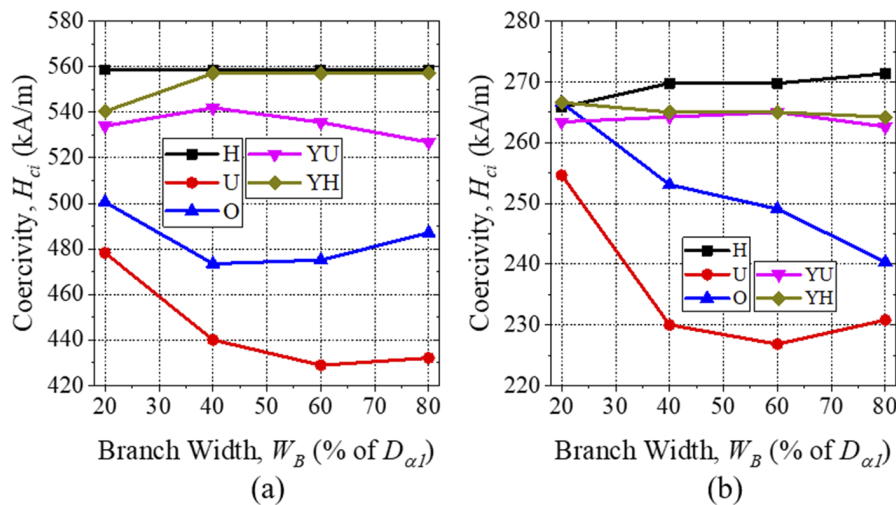


FIG. 4. H_{ci} versus W_B for $D_{\alpha 1}$ of (a) 10 nm and (b) 25 nm.

TABLE I. Recommended alnico structures for high coercivity.

Parameter	H-shaped	U-shaped	O-shaped	YH-shaped	YU-shaped
Branch length, L_B	Long/Short	Short/Short	Short/Short	Long/Any	Long/Any
Branch thickness, T_B	Any/Any	Thin/Thin	Thin/Thin	Thin/Any	Thin/Any
Branch width, W_B	Any/Any	Short/Short	Short/Short	Mid-long/Short	Mid-long/Mid-long

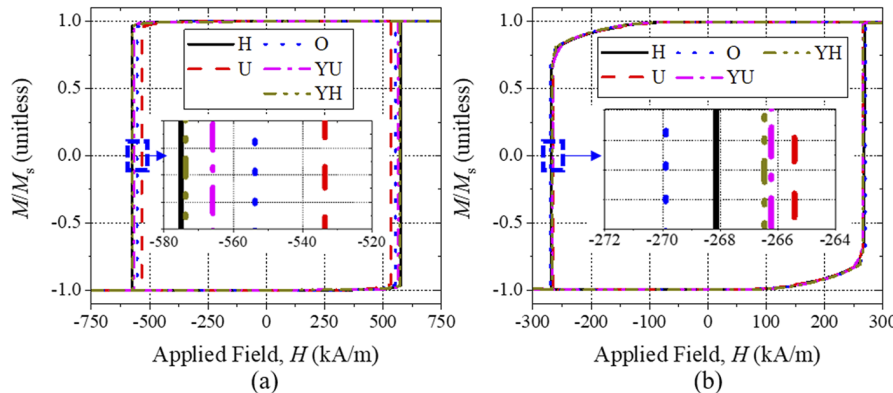


FIG. 5. Normalized M-H hysteresis loop of five structures showing highest H_{ci} for $D_{\alpha 1}$ of (a) 10 nm with branch dimensions for H-, YH-, and YU- ($L_B: 20$ nm, $T_B: 15$ nm, $W_B: 4$ nm), U- and O- ($L_B: 10$ nm, $T_B: 15$ nm, $W_B: 2$ nm), and (b) 25 nm with branch dimensions for H-, YH-, and YU- ($L_B: 10$ nm, $T_B: 65$ nm, $W_B: 15$ nm), U- and O- ($L_B: 10$ nm, $T_B: 15$ nm, $W_B: 5$ nm).

is also attributed to the in-plane spin orientation of the branch, as explained above.

Thus, it can be concluded that the structure having a branch on the bottom demands thinner T_B , while any T_B for the structures having branch on the middle for both rotations.

C. Branch width

Figure 4 shows the effects of W_B on H_{ci} of five alnico structures, having L_B of 15 nm and T_B of 30 nm at $D_{\alpha 1}$ of 10 and 25 nm. For $D_{\alpha 1}$ of 10 nm, the H-shaped alnico's H_{ci} remains constant at 558.7 kA/m, while H_{ci} of the YH-shaped structure first increases from 540.3 to 557 kA/m and remains constant as W_B increases. For the U- and O-shaped structures, a positive quadratic trend is observed for H_{ci} , while a negative quadratic trend is observed for the YU-shaped structure. For $D_{\alpha 1}$ of 25 nm, similar trends are observed. These trends are attributed to change in E_{ex} with respect to W_B .

These results suggest short W_B for the U- and O-shaped structures, any W_B for the H-shaped structure, and mid-long W_B for the YU-shaped structures for both rotations. For the YH-shaped structures, the branch with mid-long W_B for coherent rotation and short W_B for curling is demanded.

D. Optimal alnico structure and performance comparison between structures

Table I summarizes the recommended branch geometries for each alnico structure when α_1 -phase rod experiences coherent rotation and curling. Fig. 5 illustrates the normalized M-H hysteresis loop of each alnico structure with optimal branch dimensions exhibiting the highest H_{ci} for both rotations. Accordingly, the H-, U-, O-, YU-, and YH-shaped structures can realize H_{ci} of 575,

533, 553.9, 565, and 573 kA/m, respectively, when the α_1 -phase rod experiences coherent rotation. For curling, the H-, U-, O-, YU-, and YH-shaped structures can realize H_{ci} of 268.2, 265.8, 270.6, 266.6, and 266.6 kA/m, respectively.

The simulation results also show that high H_{ci} is observed for the O-shaped structure, compared to that of the U-shaped structure for all branch geometries. This is mainly attributed to the formation of T_B . As Fig. 3(a) shows, H_{ci} of the U- and O-shaped structures are the same when the U-shaped structure has half of T_B of the O-shaped structure. This is because when T_B equals 30 nm, the U-shaped structure has a 30 nm thick branch on the bottom, while the O-shaped has a 15 nm thick branch on the bottom and top (net T_B of 30 nm). The simulation results suggest that fabricating thin T_B in the direction of H_{app} is recommended to realize high H_{ci} .

In overall, alnico structure with the branch on the middle Z-axis for the coherent rotation and O-shaped alnico structures for the curling are highly recommended to realize a high H_{ci} .

IV. CONCLUSIONS

The effects of various branches' geometry and dimensions of five different alnico structures on coercivity (H_{ci}) were evaluated for coherent rotation and curling using micromagnetic simulation. The H-shaped structure demanded the branch with long length (L_B) regardless of branch thickness (T_B) and width (W_B) for coherent rotation. For curling, the structural design with short L_B , any T_B , and long W_B was demanded to realize a high H_{ci} . For the U- and O-shaped structures, fabricating alnico with short L_B , thin T_B , and short W_B is recommended for both rotations. Lastly, the YH- and YU-shaped structures demanded the branches with long L_B , thin T_B , mid-long W_B for coherent rotation and short W_B for the YH-shaped

and mid-long W_B for the YU-shaped regardless of L_B and T_B for curling.

ACKNOWLEDGMENTS

This work was supported in part by NSF-IUCRC for EVSTS under Grant No. 1650564.

AUTHOR DECLARATIONS

Conflict of Interest

The authors have no conflicts to disclose.

DATA AVAILABILITY

The data that support the findings of this study are available from the corresponding author upon reasonable request.

REFERENCES

- ¹L. Zhou, M. K. Miller, P. Lu, L. Ke, R. Skomski, H. Dillon, Q. Xing, A. Palasyuk, M. R. McCartney, D. J. Smith, S. Constantines, R. W. McCallum, I. E. Anderson, V. Antropov, and M. J. Kramer, "Architecture and magnetism of alnico," *Acta Materialia* **74**, 224 (2014).
- ²S. Zhu, J. Zhao, W. Xia, Y. Sun, Y. Peng, and J. Fu, "Magnetic structure and coercivity mechanism of AlNiCo magnets studied by electron holography," *J. Alloys Compd.* **720**, 401 (2017).
- ³Y. Zheng, L. Wu, Y. Fang, X. Huang, and Q. Lu, "A hybrid interior permanent magnet variable flux memory machine using two-part rotor," *IEEE Trans. Magn.* **55**, 8106008 (2019).
- ⁴L. Ke, R. Skomski, T. D. Hoffmann, L. Zhou, W. Tang, D. D. Johnson, M. J. Kramer, I. E. Anderson, and C.-Z. Wang, "Simulation of alnico coercivity," *Appl. Phys. Lett.* **111**, 022403 (2017).
- ⁵H. Won, Y. Hong, M. Choi, F. Yan, G. Mankey, X. Han, W. Lee, C. Yeo, J. Lee, and T. Lee, "Micromagnetic simulation of coercivity of alnico magnets," *IEEE Magn. Lett.* **12**, 7501505 (2021).
- ⁶M. R. Scheinfein, LLG Micromagnetic SimulatorTM, available at <http://llgmicro.home.mindspring.com>.